WuXi AppTec Bone Metastasis Platform to Evaluate Prophylaxis and Treatment

WuXi AppTec, WuXi Biology, Oncology & Immunology Unit

2022.05

OncoWuXi Newsletter

Outline

- **Bone metastases**
  1. Metastases and syndrome
  2. Diagnosis and treatment
- **WuXi AppTec bone metastases platform**
  1. Bone metastases model list
  2. Comparison of bone metastasis model establishment strategies
  3. Bone metastasis model data
  4. Treatment evaluation case study

Bone metastases and syndrome

Bone metastases refer to cancer cells migration and colonization from primary site to bones. It could occur in almost all cancers types, but are particularly likely in breast, lung, prostate, kidney, melanoma, ovarian, and thyroid.

The common sites for bone metastases include spine, pelvis, femur, humerus, ribs, and the skull. The metastases could cause signs and symptoms like bone pain, broken bones, urinary incontinence, bowel incontinence, weakness in the legs or arms, high levels of calcium in the blood (hypercalcemia), which can cause nausea, vomiting, constipation and confusion.

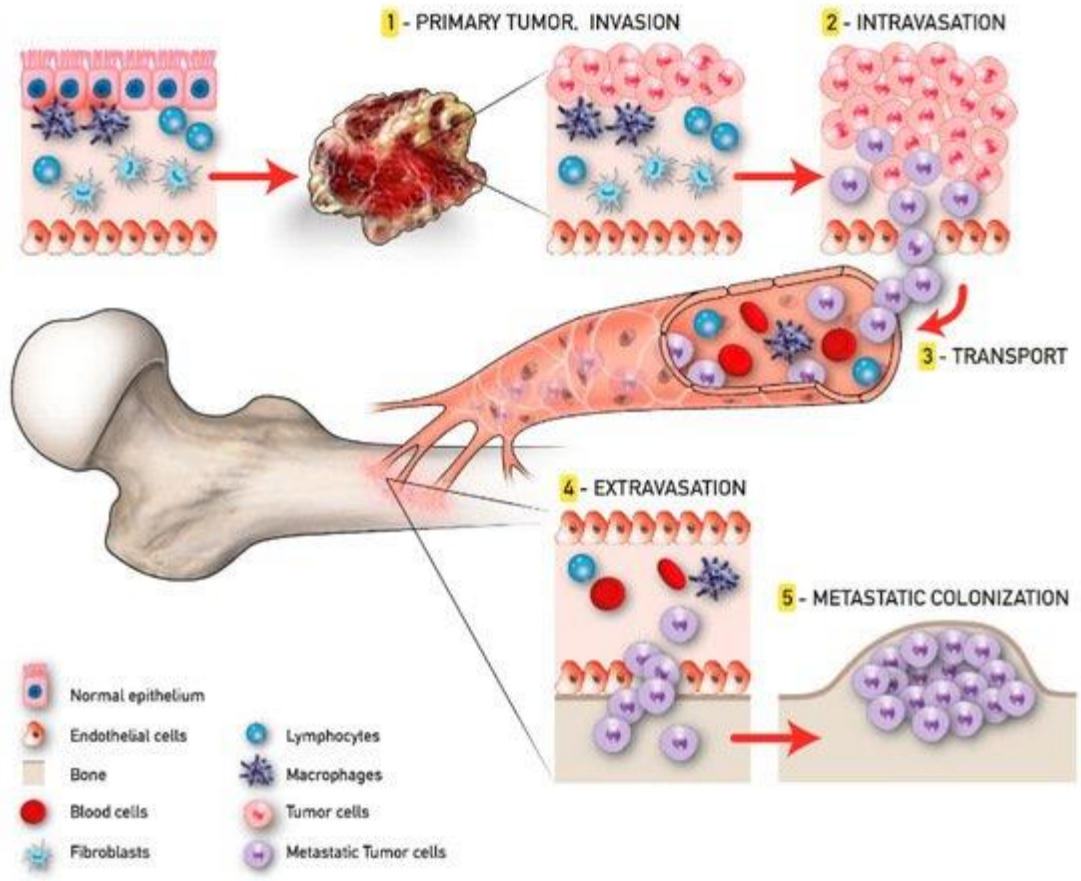

Trends in Bone Metastasis Modeling Cancers 2020, 12(8), 2315

Diagnosis and treatment

Currently clinical therapeutic strategy of bone metastatic is mainly systemic medicines, which kill cancer cells throughout the entire body:

- Chemotherapy
- Hormonal therapy, commonly used in prostate cancer and breast cancer bone metastases.
- Targeted therapies, like TKI targeting VEGFR2, MET, KIT and RET.

Some bone-modifying agents aimed at slowing bone resorption were, like bisphosphonates and RANK/RANKL inhibitors. Other bone-modifying agents under investigation include cathepsin K inhibitors, Src inhibitors, TGFβ blockers, C-X-C motif chemokine receptor type 4 (CXCR4) inhibitors, and αvβ3 integrin antagonists.

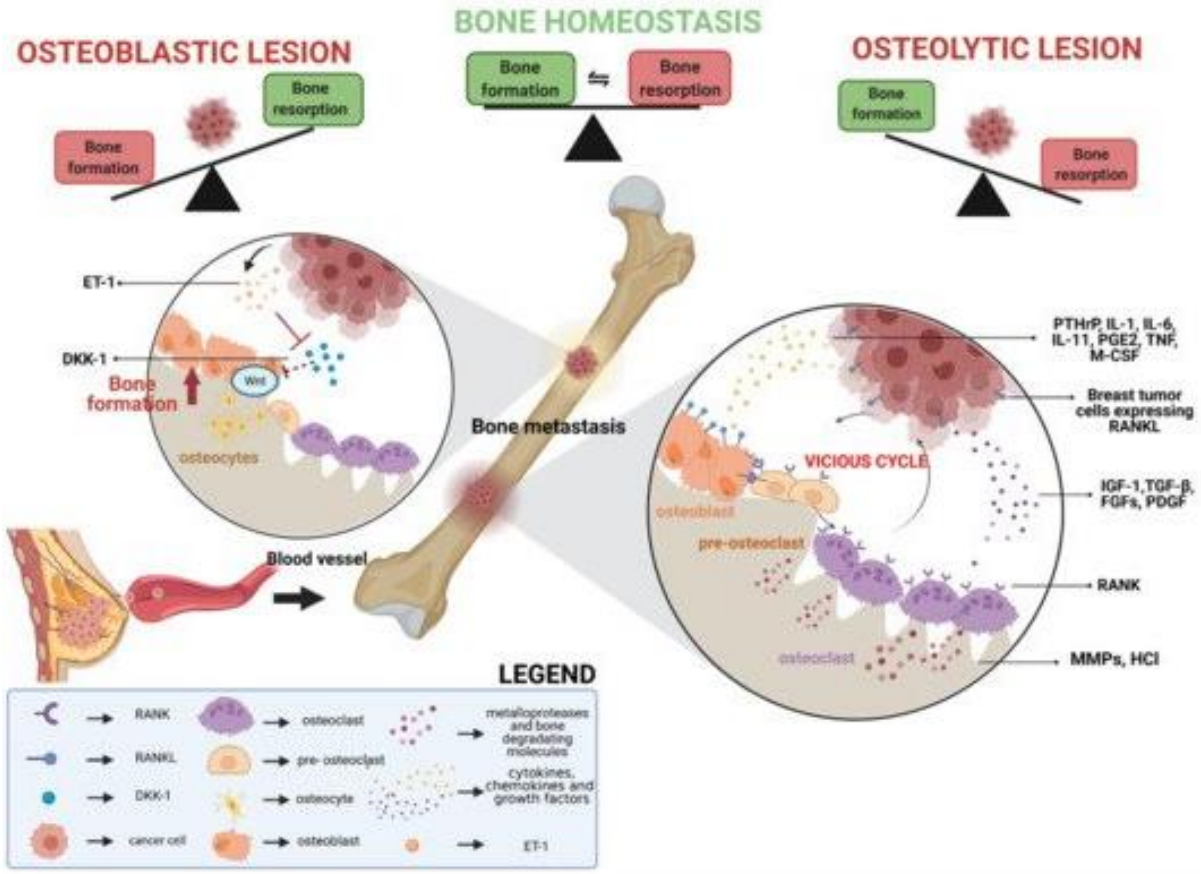

Breast Cancer with Bone Metastasis: Molecular Insights and Clinical Management Cells 2021, 10(6), 1377

WuXi AppTec bone metastases platform

- WuXi AppTec provides you with a platform for evaluating prophylaxis and treatment therapy of bone metastases.
- Currently established highly metastatic cancers types are as follows, including multiple popular targets, which is also convenient for evaluating immunotherapy, combination therapy, etc.

Cell name	Cancer type	Injection method	Type	Metastatic/target organs	Targets	Page
NCI-H1373	Lung	intraosseous	Ectopic injection	Bone and Lung	KRAS	7
NCI-H358	Lung	intraosseous	Ectopic injection	Bone	KRAS	8
MDA-MB-231	Breast	intraosseous	Ectopic injection	Bone and lung	TNBC	9
MDA-MB-231	Breast	Intra-cardiac	Metastasis	Bone and lung	TNBC	10
MDA-MB-231	Breast	Intra-caudal arterial	Metastasis	Bone	TNBC	11
JIMT-1-luc-gfp	Breast	Intra-caudal arterial	Metastasis	Bone	HER-2	12
xJIMT-1-luc-gfp*	Breast	Intra-caudal arterial	Metastasis	Bone	HER-2	13-17

**xJIMT-1-luc-gfp are derived from JIMT-1 hind limb metastasis from intra-caudal arterial tumor (at WuXi AppTec).*

Comparison of bone metastasis model establishment strategies

- Our platform could simulate the comprehensive process of metastases through a variety of different modeling strategies to meet your needs for target validation, therapy evaluation.

	Inoculation route	intra-cardiac	intravenous	intra-caudal arterial	intraosseous	orthotopic
Metastasis Formation	metastasis stages modeling from	circulation	circulation	circulation	established bone metastasis	primary tumor
	metastasis rate to hind limbs	***	**	****	NA	*
	tumor growth rate in bone	**	*	**	***	*
	tumor volumes in bone	*	*	**	**	**
	other organs macrometastases	lung, liver and brain	lung and liver	vesicular gland	soft tissues	lung, spine and jaw
Model Operations	surgery	Y	N	N	N	Y
	operation	professional	easy	easy	hard	medium
	mechanical disruption	heart	NA	NA	bone and ligaments	corresponding organs
	lethality	high	low	low	low	low
	some reported cell lines	MDA-MB-231, MCF-7, PC-3, RM1	MDA-MB-231, MCF-7, PC-3, B16	MDA-MB-231, MCF-7, PC-3, 786-O, 143B, E0771, 4T1	MDA-MB-231, MCF-7, PC-3	4T1

*Rate and tumor volume are compared among aforementioned routes, * slow/small, **** fast/large.*

NCI-H1373-luc model

Intraosseous

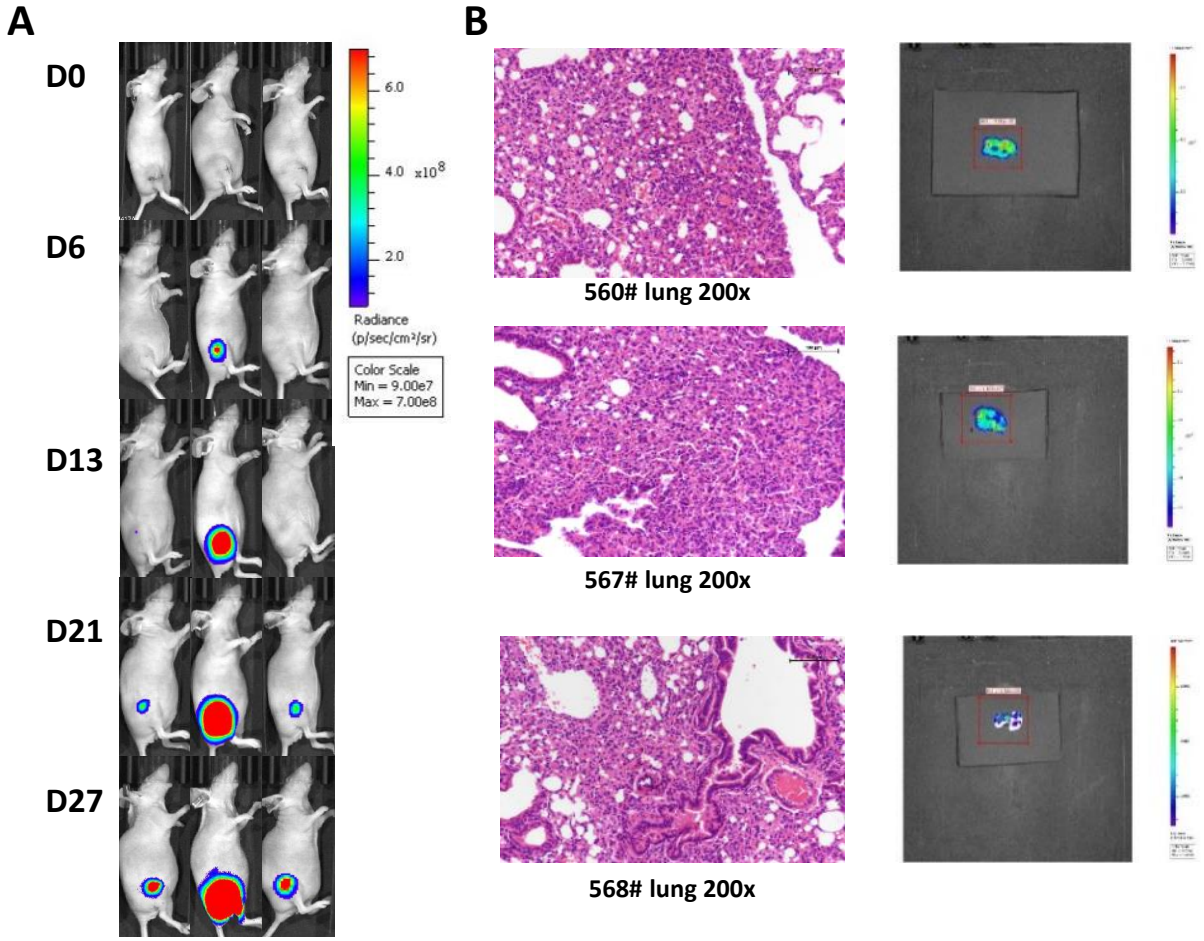

Figure: NCI-H1373-luc cells were injected into the femoral cavity of female BALB/c nude mice. **(A)** Bioluminescent imaging of the mice (High cell density, n=3). **(B)** HE imaging of the mice. **(C)** Growth curve of Bioluminescence value.

NCI-H358-luc model

Intraosseous

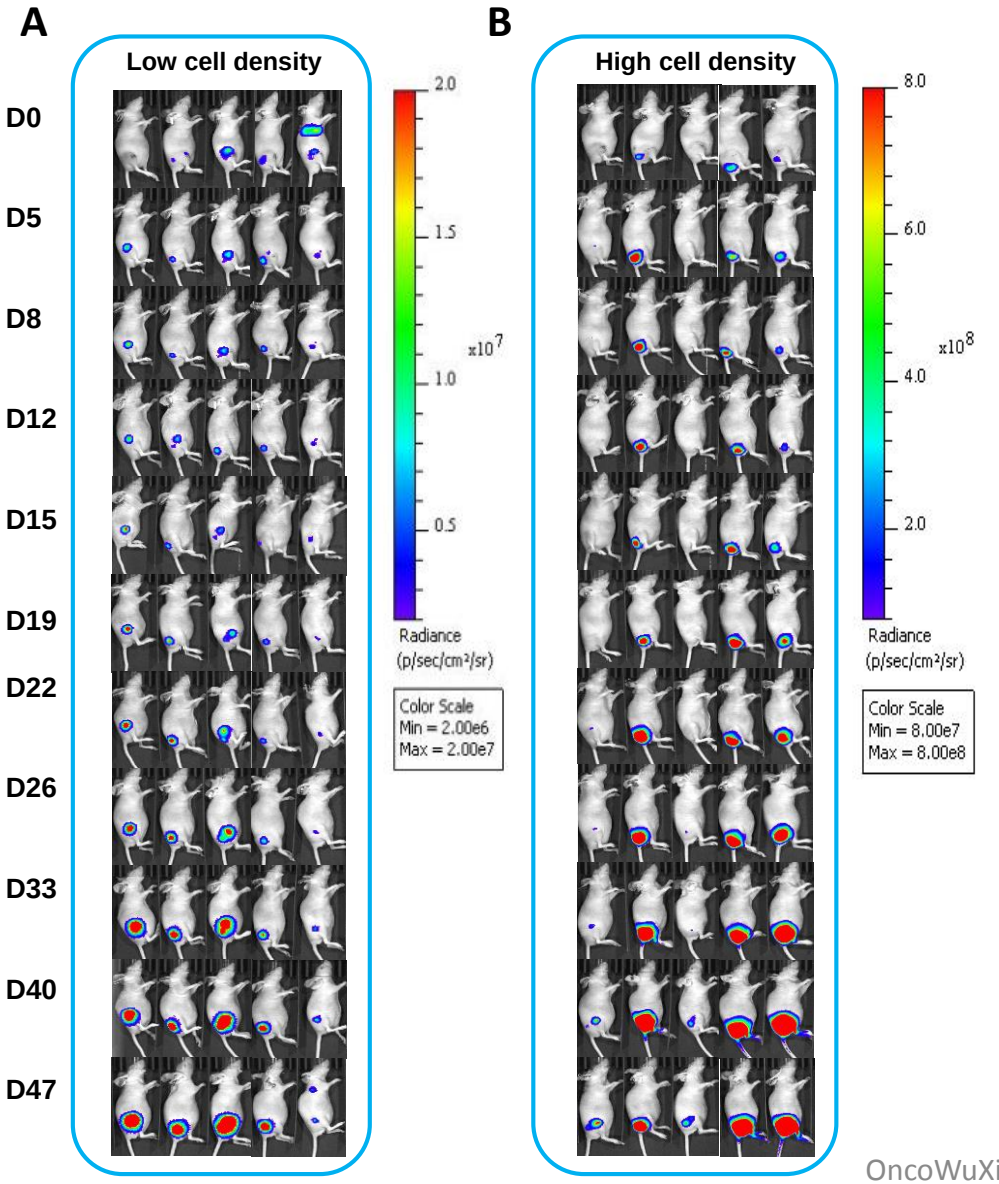

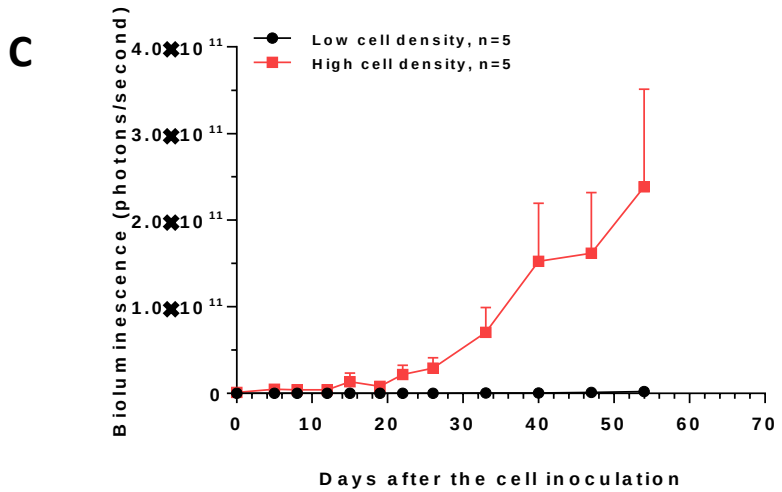

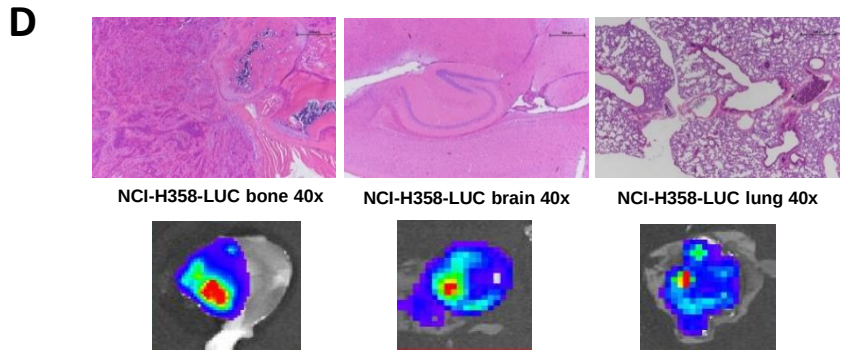

Figure: NCI-H358-luc cells were injected into the femoral cavity of female BALB/c nude mice. **(A)** Bioluminescent imaging of the mice (Low cell density, n=6). **(B)** Bioluminescent imaging of the mice (High cell density, n=6). **(C)** Growth curve of Bioluminescence value. **(D)** HE image of model.

MDA-MB-231-luc model

Intraosseous

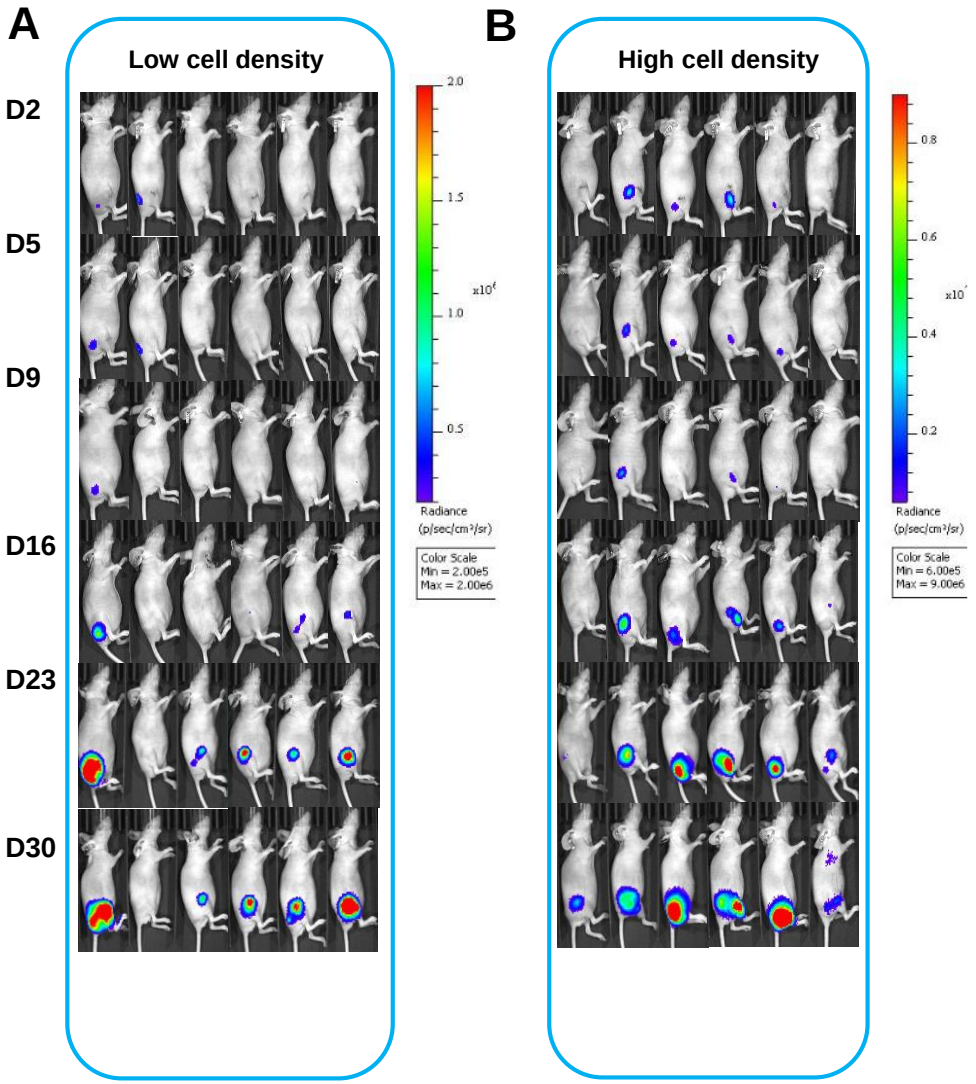

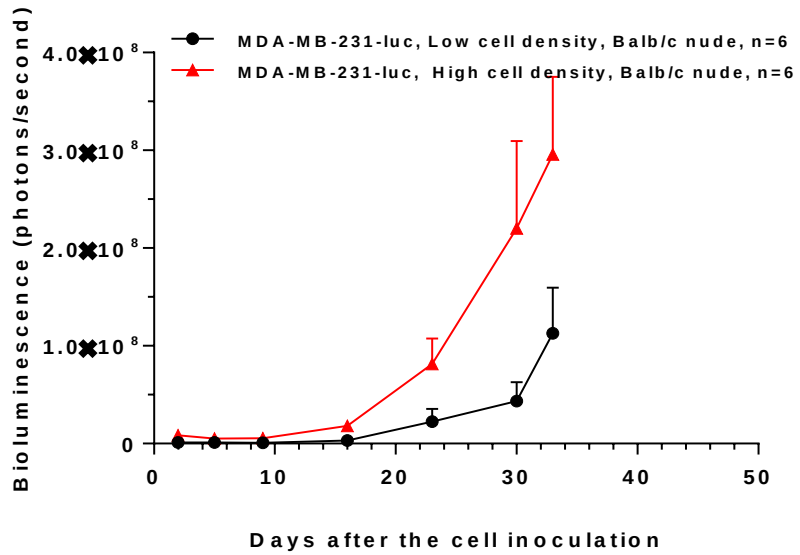

Figure: MDA-MB-231-luc cells were injected into the femoral cavity of female BALB/c nude mice. **(A)** Bioluminescent imaging of the mice (Low cell density, n=6). **(B)** Bioluminescent imaging of the mice (Low cell density, n=6). **(C)** Growth curve of Bioluminescence value.

MDA-MB-231-luc model

Intra-cardiac

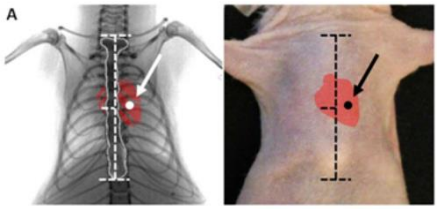

Left Ventricle injection

Campbell, JP, et al. Models of Bone Metastasis. *J. Vis. Exp.* (67), e4260 10.3791/4260, DOI : 10.3791/4260 (2012).

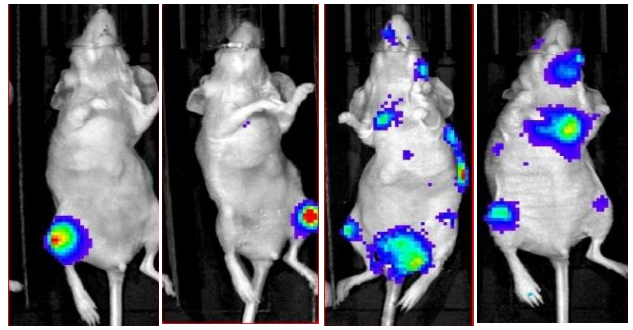

Lower Jaw | Leg Bone | Rib | Lung& Heart

Normal Tissue (leg)

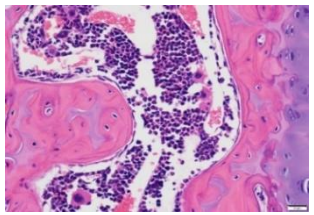

Tissue with Metastasis

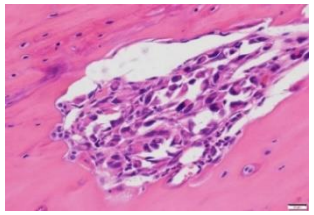

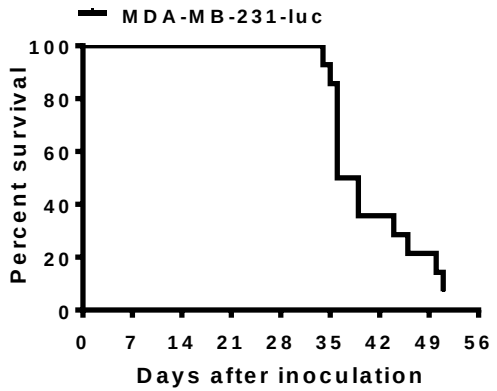

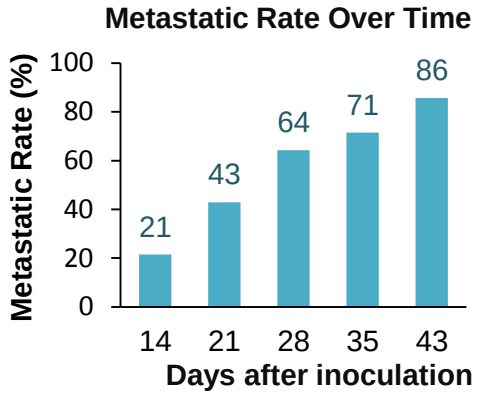

The bones are one of the most common sites of breast cancer metastases

- MDA-MB-231-luc were injected into the left ventricle to establish bone metastasis models
- Survival and metastatic rate can act as observation outputs together with bioluminescent signal increasing.

MDA-MB-231-luc model

Intra-caudal arterial

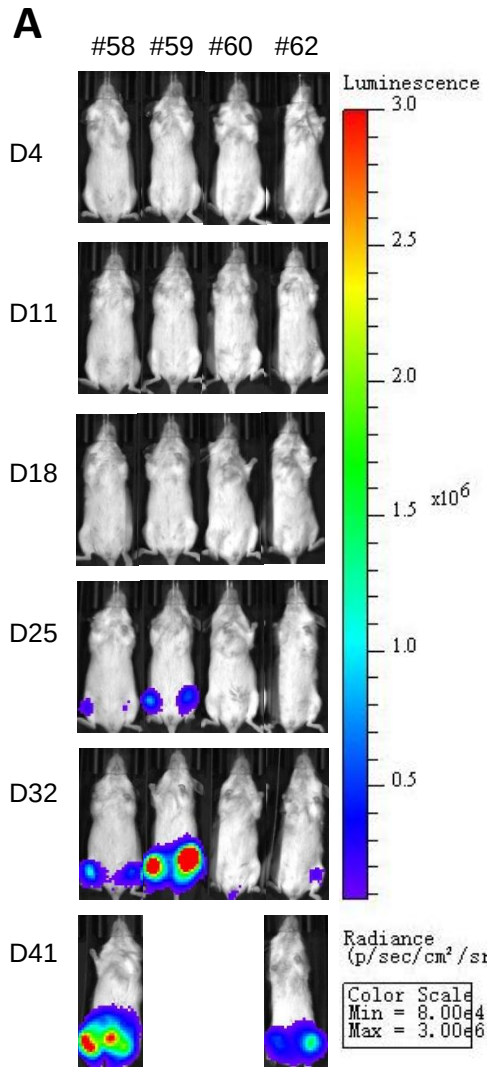

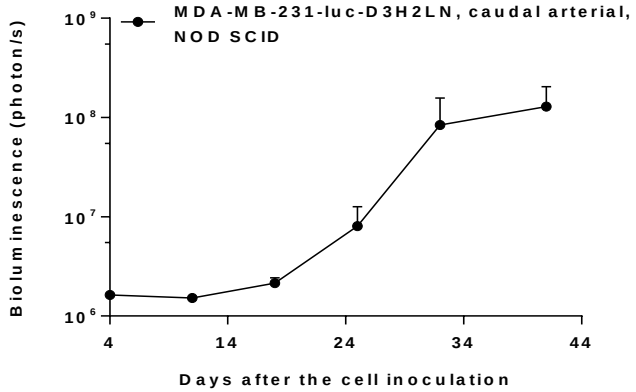

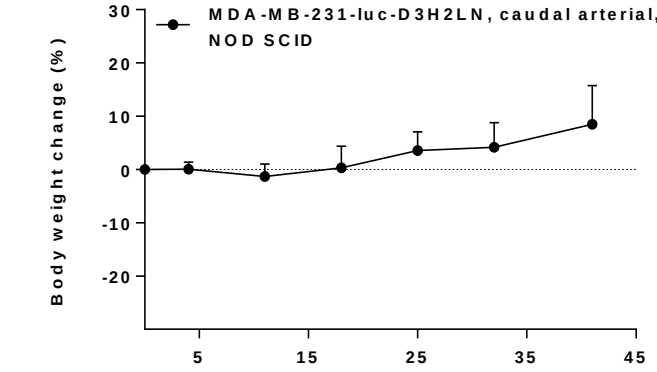

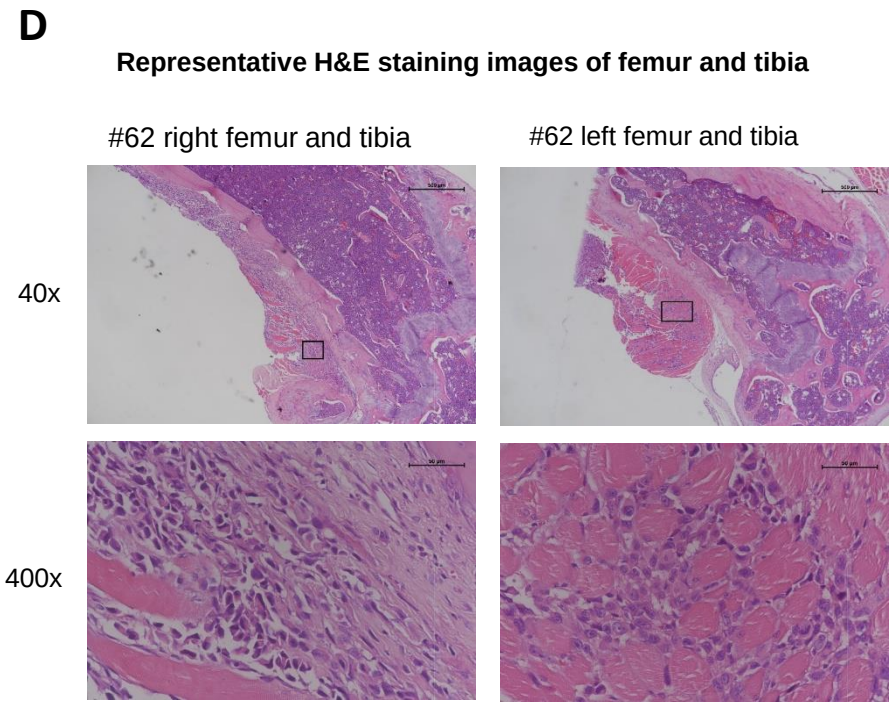

Figure: MDA-MB-231-luc cells were intra-caudal arterially injected to NOD SCID mice to establish breast cancer femur and tibia specific metastasis model. **(A)** Images of mice with metastasis bioluminescent (BLI) signals on legs. Bone metastasis is 100% (4 in 4). **(B)** Average BLI signal increase after inoculation. **(C)** Average body weight change after inoculation. **(D)** Representative H&E staining images of femur and tibia. Mouse #58 is sacrificed to collected tumor cells in bones, mouse #62's femurs and tibias were analyzed by H&E staining. Tumor cells metastasized to leg, clustered in muscles and scattered in bone marrows, causing thickness change of bones.

JIMT-1-luc-gfp model

Intra-caudal arterial

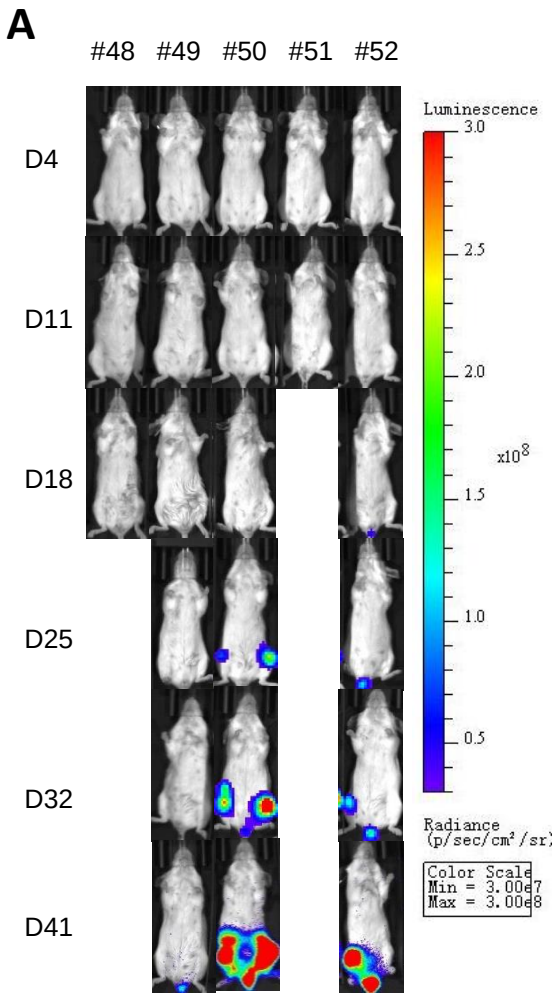

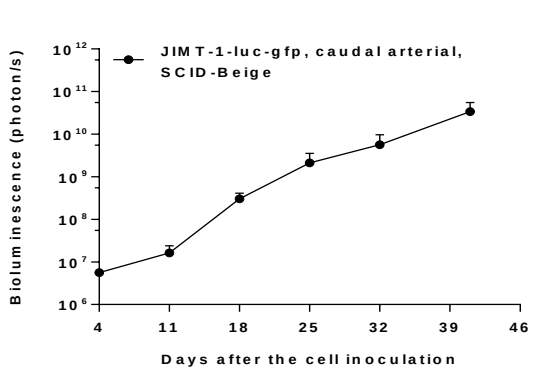

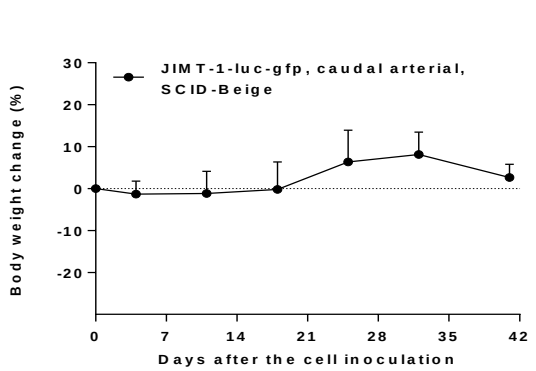

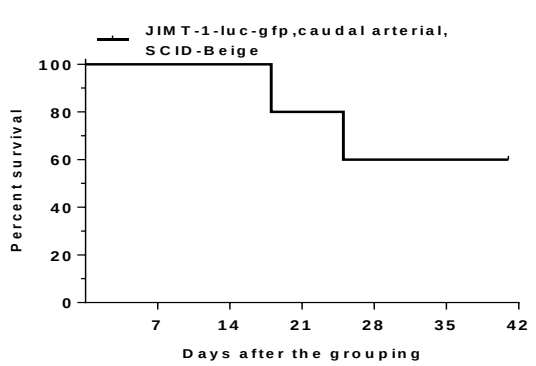

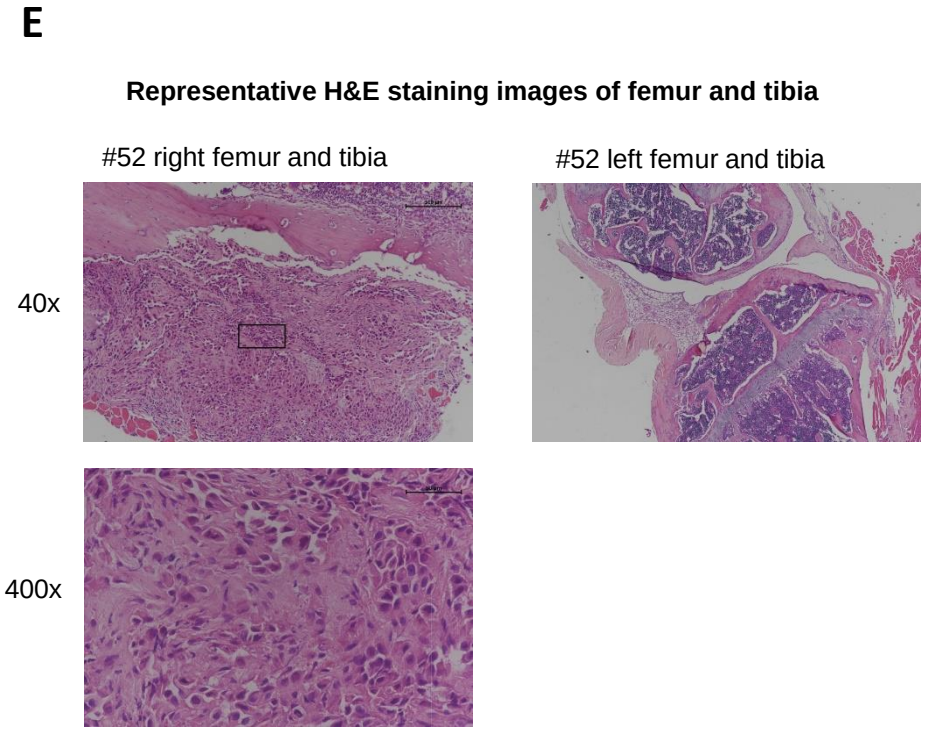

Figure: JIMT-1-luc-gfp cells were intra-caudal arterially injected to SCID Beige mice to establish breast cancer femur and tibia specific metastasis model. **(A)** Images of mice with metastasis bioluminescent (BLI) signals on legs. Bone metastasis is 80% (4 in 5). **(B)** Average BLI signal increase after inoculation. **(C)** Average body weight change after inoculation. **(D)** Survival curve of 5 mice. Mouse #50 is sacrificed to collected tumor cells in bones, mouse #52's femurs and tibias were analyzed by H&E staining. **(E)** H&E staining images of femur and tibia. Tumor cells metastasized to leg, clustered in muscles and scattered in bone marrows, causing thickness change of bones.

xJIMT-1-luc-gfp model with T-DM1

Case study

1. Model establishment

Group	N	Mouse strain	Tumor inoculation	
			Model	Route
1	15	SCID Beige	xJIMT-1-luc-gfp	Intra-caudal arterial

2. Efficacy study

a. In-life study design

Group	N	Mouse strain	Tumor inoculation		Evaluation		
			Model	Route	Treatment	Dosage	Schedule
1	8	SCID Beige	xJIMT-1-luc-gfp	Intra-caudal arterial	Vehicle	-	Twice, i.v., PG-D1 and PG-D22
2	8	SCID Beige	xJIMT-1-luc-gfp	Intra-caudal arterial	T-DM1	15 mpk	Single, i.v., PG-D22
3	8	SCID Beige	xJIMT-1-luc-gfp	Intra-caudal arterial	T-DM1	15 mpk	Twice, i.v., PG-D1 and PG-D22

b. ex vivo study

- Pathology analysis of bone metastases

c. Readout

- Tumor growth curve
- Survival curve
- Metastases rate
- Pathology review

xJIMT-1-luc-gfp model

Intra-caudal arterial

A

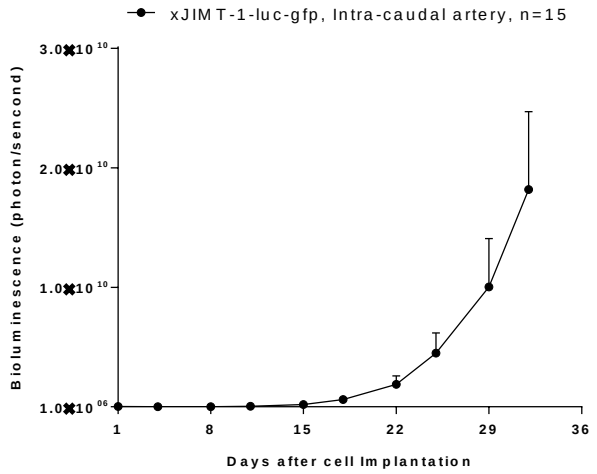

B

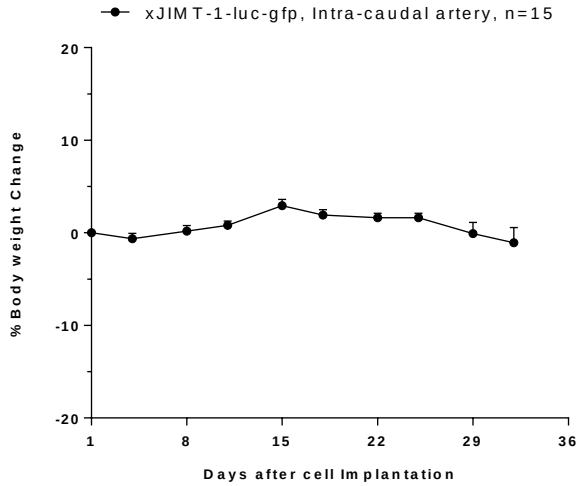

C

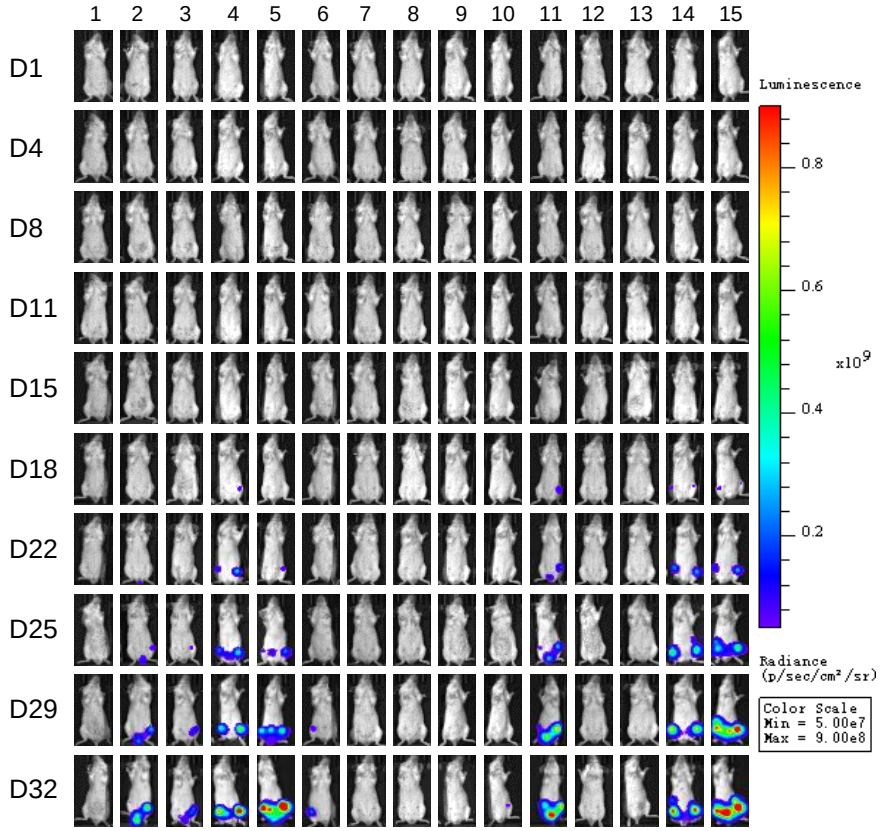

Figure: xJIMT-1-luc-gfp cells were injected into the SCID Beige mice through the caudal artery. Bioluminescence values were measured at various days. **(A)** Mean bioluminescence signal intensity of each group was quantified from each animal. Signals are plotted against days after treatment (n=15); **(B)** Body weight growth curve during the experiment (n=15); **(C)** Bioluminescent imaging of mice over 32 days (n=15). Bioluminescence signal were found in leg from PG-D18. The signal gradually increased and was clearly concentrated on the hind limbs, both tibias and femurs, signals were also found on the abdomen and the tail base.

xJIMT-1-luc-gfp model

Intra-caudal arterial

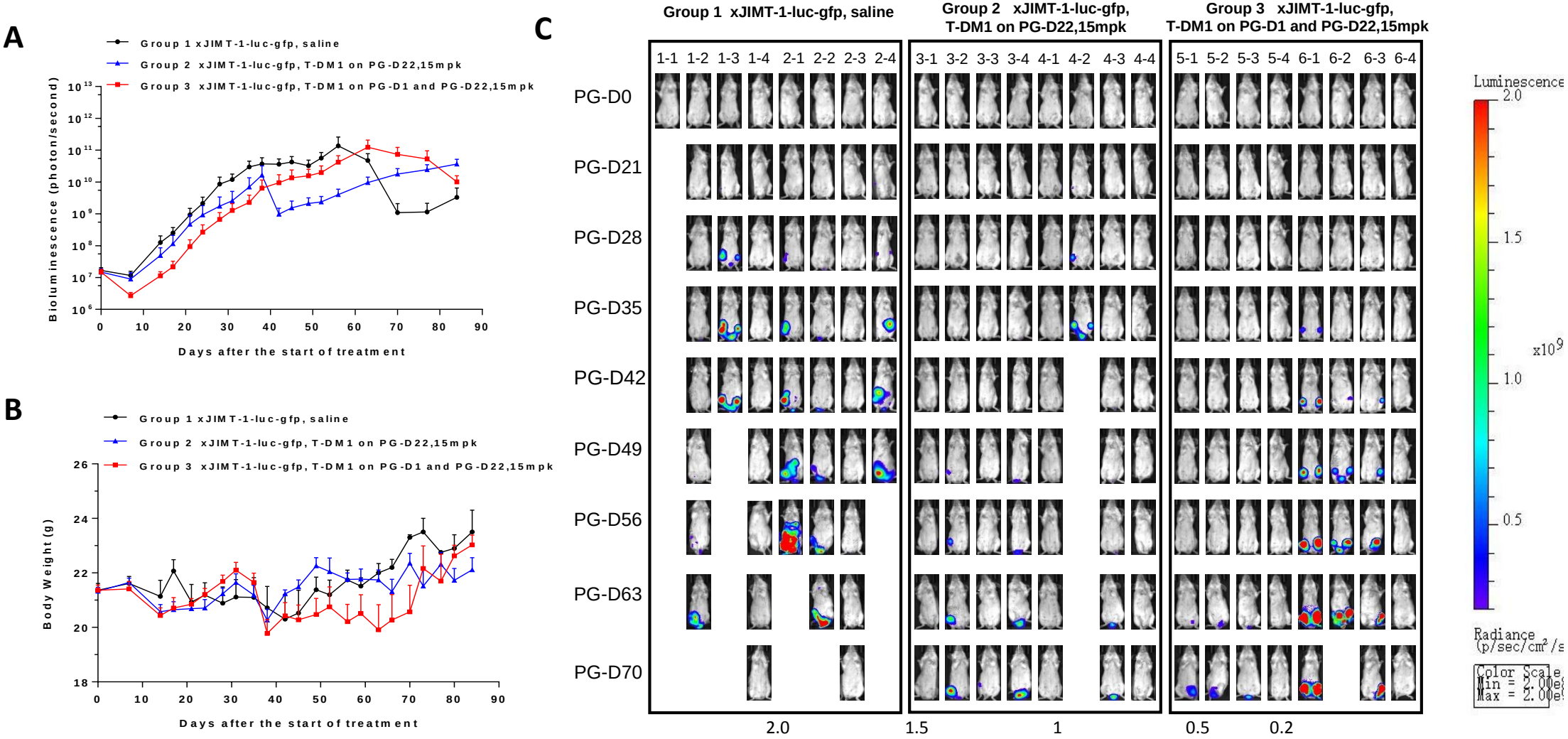

Figure: (A) Fluorescence signal intensity of each group was quantified from each animal plotted and is shown as a function of the number of days after the start of treatment (n=8). **(B)** Body weight growth curve during the experiment (n=8). **(C)** Bioluminescent imaging of mice over 70 days (n=8). Fluorescence signal were found in leg from PG-D21. The signal gradually increased and was clearly concentrated on the hind limbs, both tibias and femurs, signals were also found on the abdomen and the tail base.

xJIMT-1-luc-gfp model

Intra-caudal arterial

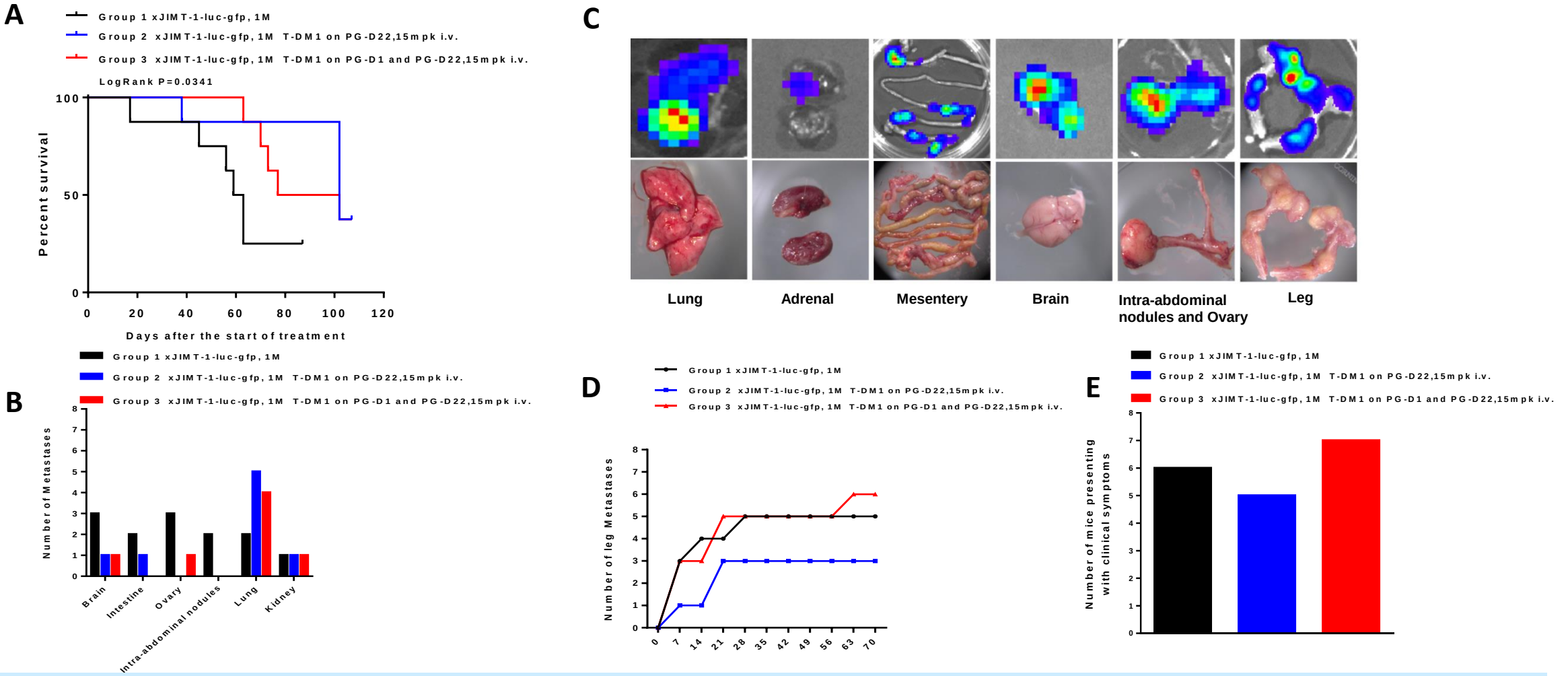

Figure: (A) Survival curve during the experiment. T-DM1 dosing in Group 2 and Group 3 prolongs the life span of mice. **(B)** Total number of mice with metastases of organs in each group. Organ specific metastases were found in most mice, the organ with the highest metastasis rate is the lung. **(C)** Anatomical and bioluminescence images of representative metastasis organs from PG-D38 to PG-D45. Besides hind limbs, metastases can occur in different organs of individual mice. **(D)** Take rate of hind limb metastases in each group during the experiment over 70 days. 75% mice in vehicle group got hind limb metastasis by day 28. **(E)** Total number of mice with clinical symptoms in each group during the experiment over 107 days. Clinical symptoms gradually appeared, including redness, swelling, heat, and dysfunction of the hind limbs. Less severe clinical symptoms found in the mice of Group 3 compared to Group 1.

xJIMT-1-luc-gfp model

Intra-caudal arterial

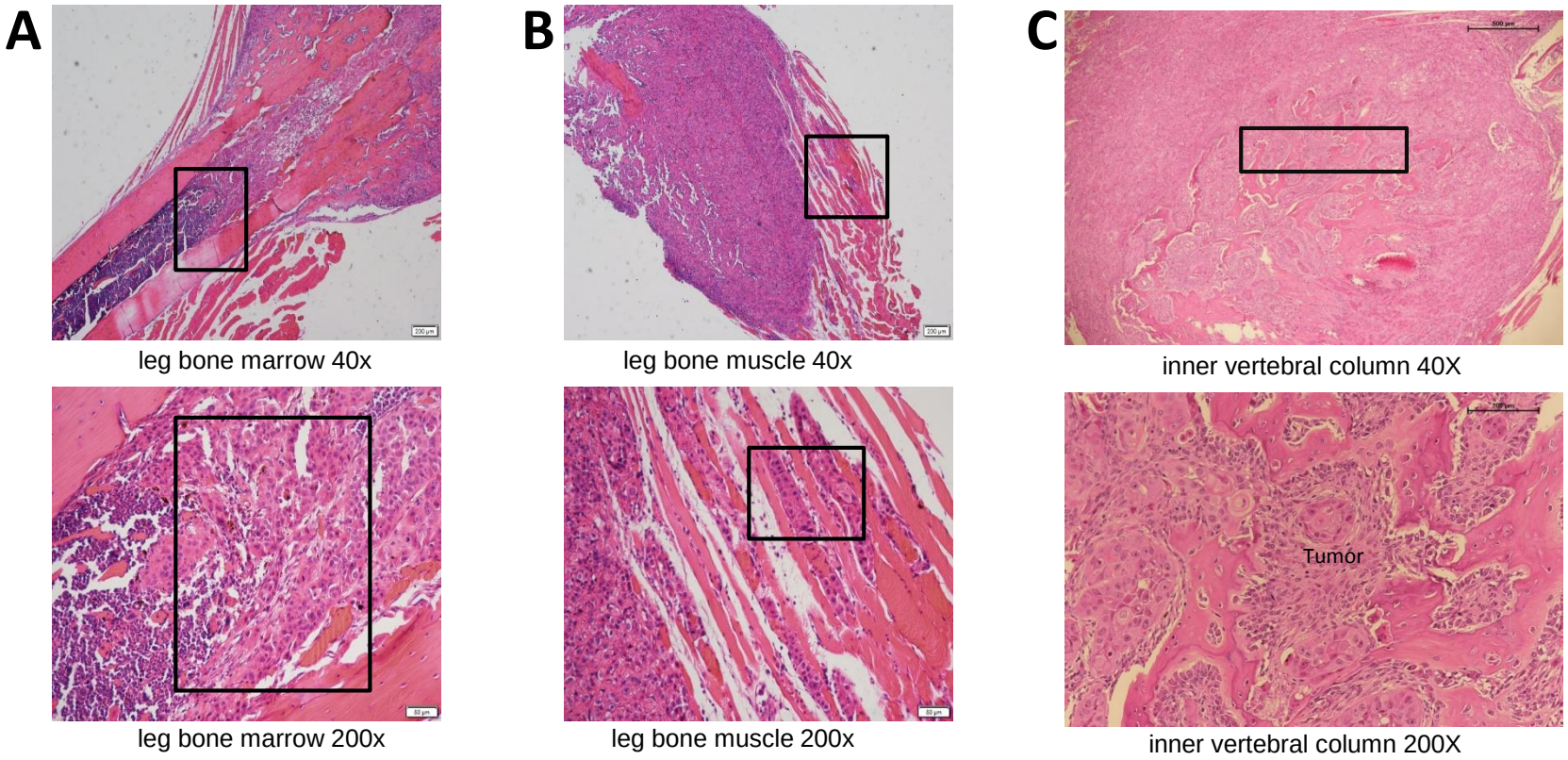

Figure: Representative H&E staining images of bone metastasis. **(A).** Metastatic tumor cell in bone marrow. Mouse was euthanized on PG-D38, tibias and femurs were taken for H&E staining. Tumor cell migrated to leg, colonized and invaded in leg bone marrow. Bone structure was destructed. **(B).** Metastatic tumor cell in bone muscle. Mouse was euthanized on PG-D38, muscle from hind limb was taken for HE staining. Leg muscle was damaged by metastatic tumor. **(C)**. Metastatic tumor cell in vertebral column. Mouse was euthanized on PG-D63, vertebral column was taken for H&E staining. Tumor cell migrated to vertebral column, and colonized on bone trabecula.

OUR COMMITMENT

Improving Health. Making a Difference.

For questions and requests, please email to info_onco@wuxiapptec.com

ONCO

WuXi

https://onco.wuxiapptec.com